

# Ultrafast dynamics of charge density waves in $4H_b$ -TaSe<sub>2</sub> probed by femtosecond electron diffraction

N. Erasmus<sup>1,\*</sup>, M. Eichberger<sup>2,\*</sup>, K. Haupt<sup>1</sup>, I. Boshoff<sup>1</sup>, G.

Kassier<sup>1</sup>, R. Birmurske<sup>2</sup>, H. Berger<sup>3</sup>, J. Demsar<sup>2</sup>, and H. Schwoerer<sup>1</sup>

<sup>1</sup>*Laser Research Institute, Stellenbosch University, Stellenbosch 7600, South Africa*

<sup>2</sup>*Department of Physics and Center of Applied Photonics,*

*University of Konstanz, 78464 Konstanz, Germany and*

<sup>3</sup>*Physics Department, EPFL CH-1015 Lausanne, Switzerland*

(Dated: November 29, 2018)

The dynamics of the photoinduced commensurate to incommensurate charge density wave (CDW) phase transition in  $4H_b$ -TaSe<sub>2</sub> are investigated by femtosecond electron diffraction. In the perturbative regime the CDW reforms on a 150 ps timescale, which is two orders of magnitude slower than in other transition-metal dichalcogenides. We attribute this to a weak coupling between the CDW carrying  $T$  layers and thus demonstrate the importance of three-dimensionality for the existence of CDWs. With increasing optical excitation the phase transition is achieved showing a second order character in contrast to the first order behavior in thermal equilibrium.

Reduced dimensionality seems to be a decisive property governing phenomena like high temperature superconductivity and charge density wave (CDW) formation. The latter is typical for quasi one- or two-dimensional metals where, in the ground state, the crystal displays a static periodic modulation of the conduction electron density accompanied by a periodic lattice displacement (PLD), both characterized by the wave vector  $\mathbf{q}_{\text{CDW}}$  [1]. The standard theory that describes the appearance of this macroscopic quantum state was formulated by Peierls [2]. By considering a one dimensional metal he has shown that the divergent static electronic susceptibility at a wave vector  $\mathbf{q} = 2\mathbf{k}_F$  gives rise to an instability of the electronic system against perturbations at this wave vector. This so called Fermi surface nesting lowers the frequencies of  $\mathbf{q} = 2\mathbf{k}_F$  phonons, which will eventually evolve into a static lattice displacement. From that band gaps at  $\pm \mathbf{k}_F$  result, which reduce the total electronic energy. If the elastic energy cost to modulate atomic positions is lower than the electronic energy gain, the CDW state is the preferred ground state. Recently, this classical picture has been challenged [3–5], since (a) the nesting condition derived from the topology of the Fermi surface ( $2\mathbf{k}_F$ ) and the observed CDW modulation vectors ( $\mathbf{q}_{\text{CDW}}$ ) are not generally equal, and (b) the diverging susceptibility at  $\mathbf{q} = 2\mathbf{k}_F$  is exceedingly fragile with respect to temperature, scattering or imperfect nesting [3]. Contrasting the standard Fermi surface nesting scenario the transition from the metallic into a CDW state was argued to occur due to strong  $\mathbf{q}$ -dependent electron-phonon coupling [3], particularly in transition-metal dichalcogenides [4].

Only the concerted interplay of electronic and lattice degrees of freedom make the CDW formation possible. The two modulations can be individually examined by scanning tunneling microscopy [6], angular resolved photoemission spectroscopy [5] and electron, x-ray or neutron diffraction techniques [7]. In thermal equilibrium,

the gap in the electronic spectrum and the atomic displacement amplitude ( $A$ ) present different projections of the same order parameter [1]. Adding femtosecond temporal resolution to the experiment enables investigation of their dynamical behavior. Since the electronic system can be perturbed on timescales much faster than the characteristic lattice vibration periods these femtosecond real-time techniques enable studies of the interplay between these two components of the order parameter. Studies of coherently driven collective modes [8–10], photoinduced phase transitions [11–14] as well as manipulation of the order parameter [15, 16] have been performed with femtosecond resolution in both quasi one- and two-dimensional CDW compounds. By tracking the photoinduced changes in optical properties or in photoelectron emission spectra, information about the transient changes in the electronic subsystem of the CDW can be obtained, while the lattice dynamics can be deduced only indirectly [10]. With the recent development of time-resolved structural probes, such as ultrafast x-ray [17–19] and electron diffraction [20–22] techniques, structural dynamics in solids are becoming experimentally accessible [23, 24], enabling direct insight into the coupling strength between electrons and the lattice and their dynamical interplay.

In this Letter we report on systematic excitation density studies of structural dynamics in the CDW system  $4H_b$ -TaSe<sub>2</sub> in its room temperature phase. Here commensurate (C) CDWs exist in the octahedrally coordinated layers. Upon strong enough excitation the phase transition to an incommensurate (IC) high temperature CDW phase can be achieved on the sub picosecond timescale. By means of femtosecond electron diffraction we were able to directly probe the structural order parameter dynamics following photoexcitation with near-infrared femtosecond optical pulses. Resolving the CDW suppression dynamics on the sub picosecond timescale we demonstrate the importance of specific strongly cou-

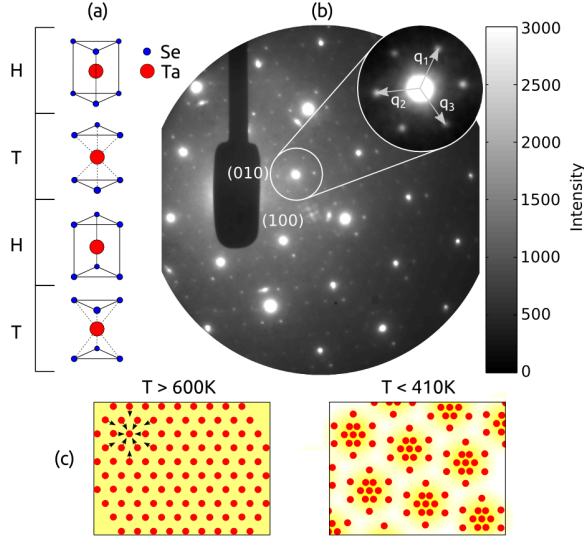


FIG. 1. Crystal structure and charge density waves in  $4H_b$ -TaSe<sub>2</sub>: Panel (a) depicts the alternating stacking of  $T$  and  $H$  layers of the unit cell. The equilibrium diffraction pattern of the studied sample is shown in panel (b). Here two primitive lattice points are indexed. The insert shows the six CDW satellites around each Bragg peak. Panel (c): above 600 K (metallic phase) the Ta ions are hexagonally arranged. Below  $T_C = 410$  K the Ta ions of the  $T$  layers are commensurately  $(\sqrt{13} \times \sqrt{13})$  modulated: twelve ions cluster around one central ion to form a commensurate PLD. The conduction electron density (shaded) is modulated accordingly.

pled phonons for the disappearance of the CDW. Moreover, the CDW reformation dynamics is found to be dramatically slower than in recently studied  $1T$ -TaS<sub>2</sub> [23] and  $1T$ -TiSe<sub>2</sub> [24] implying the importance of three-dimensionality for the existence of CDW order. Finally, by studying the non-equilibrium CDW state generated by optical perturbation as a function of excitation density we demonstrate the change of order of the C-IC phase transition: while in thermal equilibrium it is of strongly first order the ultrafast optically induced phase transition is of second order type.

$4H_b$ -TaSe<sub>2</sub> is a quasi two-dimensional crystal consisting of covalently bound three atom thick planar layers of type Se-Ta-Se which are weakly bound to each other along the crystallographic  $c$ -axis via van der Waals interaction, see Fig. 1(a). In the high temperature metallic phase  $4H_b$ -TaSe<sub>2</sub> belongs to the space group  $P6_3/mmc$  with the hexagonal lattice parameters of  $a = b = 3.455$  Å and  $c = 25.15$  Å [25]. Here, octahedrally coordinated  $T$  layers alternate with trigonal prismatic  $H$  layers, with the individual Ta atoms being aligned on top of each other along the  $c$ -axis. This structure serves as a host lattice for CDW induced modulations at lower temperatures: below 600 K an IC-CDW in the  $T$  layers is formed with  $\mathbf{q}_{CDW} = 0.265 \mathbf{a}^*$ . By further lowering

the temperature through a first order phase transition at  $T_c = 410$  K a C-CDW with  $\mathbf{q}_{CDW} = 0.277 \mathbf{a}^*$  ( $\mathbf{q}_{CDW}$  is tilted by  $13.9^\circ$  from  $\mathbf{a}^*$ ) is formed [26, 27]. The periodic lattice displacement of the charge density wave appears as  $(\sqrt{13} \times \sqrt{13})R13.9$  modulation, with no modulation vector along the  $c$ -axis [7]. The modulation, schematically shown in Figure 1 (c), is reflected in the electron diffraction pattern. Here each of the Bragg peaks of the host lattice is surrounded by six weak satellite reflections whose intensity is only a few percent of the intensity of the Bragg peaks of the host lattice, see Fig. 1(b). In both phases, C and IC, no CDW order is present in the  $H$  layer; a slight modulation therein can be assigned to elastic coupling between the two types of layers [7]. Only upon further cooling below 75 K, the  $H$  layers develop an IC-CDW which coexists with the still commensurately modulated  $T$  layers [7, 26]. Thus, the CDW in  $4H_b$ -TaSe<sub>2</sub> at room temperature presents a good approximation to a true two-dimensional CDW system.

Single crystals of  $4H_b$ -TaSe<sub>2</sub> were grown by chemical vapour transport. From the bulk crystal 90 nm thin sheets  $> 150 \mu\text{m}$  in diameter were cut along the TaSe<sub>2</sub> planes using an ultramicrotome and mounted on TEM meshes [28]. Time-resolved electron diffraction experiments were performed in transmission geometry in a collinear excitation scheme applying 200 fs near-infrared pump pulses ( $\lambda = 775$  nm) for photoexcitation, and delayed ultrashort electron pulses as probe. We used a 30 kV femtosecond electron gun with a gold photocathode, driven by 150 fs laser pulses ( $\lambda = 258$  nm) at a repetition rate of 1 kHz to produce electron bunches containing  $\sim 1000$  electrons. Their duration at the sample position was independently measured by a compact ultrafast streak camera to be 300 fs [29]. The lateral FWHM of the electron beam on the sample was  $200 \mu\text{m}$ , while its transverse coherence length was measured to be 5 nm. Variable time delay  $t_d$  between optical pump pulse and the electron probe pulse was realized with a computer controlled translation stage in the pump laser path. Accurate spatial overlap of electron and laser pulses on the sample was actively controlled by monitoring the position of the electron and laser spot and correcting the overlap with piezo driven mirrors if necessary. Diffraction patterns were detected with a pair of chevron stacked micro channel plates coupled to a phosphor screen, and imaged onto a 16 bit CCD camera. Diffraction images at different time delays were taken with 60 seconds exposure (60,000 shots). Each image with the pump laser pulse incident on the sample was followed by an identical unpumped exposure for reference. The maximum achievable temporal resolution was about 400 fs, if  $\lesssim 1000$  electrons per bunch were used. At large time-delays the data were recorded with higher numbers of electrons per pulse to increase the signal to noise ratio and decrease the acquisition time.

We have performed the experiments at room temperature and analyzed the temporal evolution of photoin-

duced changes in the intensity of the Bragg peaks and their CDW satellites at the individual diffraction orders. In all six diffraction orders both satellite and Bragg peaks showed identical temporal evolution. Thus, for the sake of increasing the signal to noise level, individual CDW and Bragg traces were averaged over all available diffraction orders [23]. The experiments were performed as a function of excitation fluence  $F$ , which was varied between 1 and 3 mJ/cm<sup>2</sup>. Since the optical beam diameter was 500  $\mu$ m and the optical penetration depth of 110 nm [30] is larger than the film thickness nearly homogenous excitation is achieved.

Four diffraction images at different time-delays at  $F = 2.6$  mJ/cm<sup>2</sup> are shown in Fig. 2(a). At this excitation density the intensity of the CDW peaks of the C-phase is completely suppressed on a sub-ps timescale, corresponding to the photoinduced C-IC phase transition. Due to the reduced PLD amplitude in the IC-phase the weak CDW peaks of the IC-phase are not resolved. Figure 2 (b) and (c) show the evolution of the changes in Bragg peak ( $I_{\text{Bragg}}$ ) and CDW satellite ( $I_{\text{CDW}}$ ) intensities for three different excitation fluences as a function of time-delay  $t_d$ . The suppression of  $I_{\text{CDW}}$  ranges from  $\approx 30\%$  at  $F = 1.7$  mJ/cm<sup>2</sup> to a complete suppression of the C-CDW order at  $F = 2.6$  mJ/cm<sup>2</sup>. As the CDW is partially suppressed,  $I_{\text{Bragg}}$  gains in intensity as the crystal is driven towards a more symmetric state, see Fig. 2(b). This process is followed by a rapid decrease of  $I_{\text{Bragg}}$  accompanied by a further reduction in  $I_{\text{CDW}}$ , which take place on the sub-ps timescale. For the perturbative regime, at  $F < 2.5$  mJ/cm<sup>2</sup>, the recovery of the CDW state is observed on the 150 ps timescale, while for  $F > 2.5$  mJ/cm<sup>2</sup> the recovery proceeds on a much longer timescale.

In order to analyze the structural dynamics we propose the following simple model. Photoexcitation of electrons and initial e-e scattering result in pronounced changes also in the electron distribution of the Ta 5d band. This process gives rise to strong modification of the interatomic potential thereby launching highly cooperative (coherent) atomic motion towards the new equilibrium positions of the high-T phase via the breathing amplitude mode of the 13 Ta atom clusters in Fig. 1(c). Thus, the PLD amplitude is suppressed as manifested by the suppression of  $I_{\text{CDW}}$  and the corresponding increase in  $I_{\text{Bragg}}$ . This timescale,  $\tau_{\text{coh}}$ , is found to be shorter than our experimental time-resolution. Following the transient increase  $I_{\text{Bragg}}$  starts to decrease on a timescale  $\tau_{\text{icoh}}$ , during which  $I_{\text{CDW}}$  gets further suppressed. This timescale is characteristic of electron-phonon relaxation processes, whereby the excited  $\mathbf{q} \neq 0$  phonons give rise to suppression of  $I_{\text{Bragg}}$  similar to the Debye-Waller effect. Similarly, the phonons which are strongly coupled to the Ta 5d electrons seem to further destabilize the CDW. Thus, we modeled the relative changes of Bragg and CDW scattering intensities

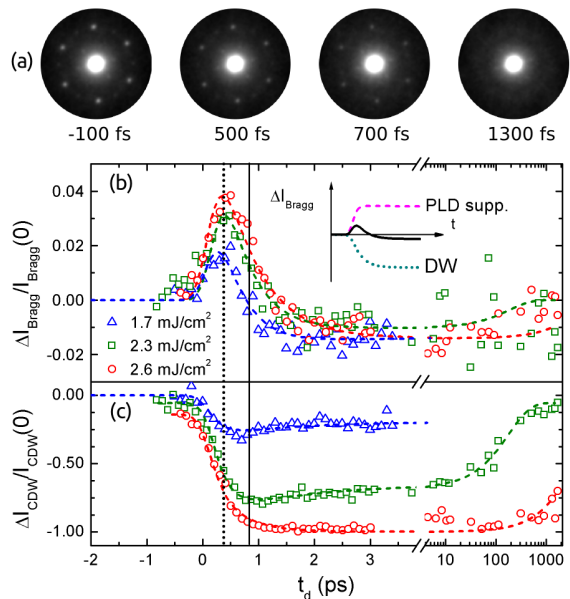


FIG. 2. Temporal evolution of the diffraction intensities. Panel (a) shows the evolution of the insert in Fig.1(b) at several pump probe delays. Panels (b) and (c) represent the transient intensity changes in the Bragg and CDW reflections at different fluences  $F$ , respectively. The dashed lines are fits to the data, see text. The vertical solid and dashed lines indicate the times of the minimum of  $I_{\text{CDW}}$  and the maximum of  $I_{\text{Bragg}}$  at  $F = 2.3$  mJ/cm<sup>2</sup>, respectively. The inset to panel (b) shows the two exponential components which in superposition (solid black) give the fit curve for the Bragg transient.

as  $C_1(1 - \exp(-t_d/\tau_{\text{coh}})) + C_2(1 - \exp(-t_d/\tau_{\text{icoh}}))$ , with  $C_1, C_2 < 0$  for the case of  $\Delta I_{\text{CDW}}(t_d)$  and  $C_1 > 0, C_2 < 0$  for  $\Delta I_{\text{Bragg}}(t_d)$ ; the latter has been sketched for clarity in inset to Figure 2 (b).

Three modes around 70 cm<sup>-1</sup> have previously been reported to show the characteristic softening of CDW amplitude modes upon warming towards  $T_c$  [31]. Since the ultimate timescale for the (coherent) suppression of the C-CDW is given by 1/4 of a period of the amplitude mode we chose  $\tau_{\text{coh}} = 150$  fs. Moreover, to fit the entire traces, the function has been multiplied by an exponential decay to account for the reformation dynamics, and convoluted with a Gaussian pulse with FWHM of 400 fs to make up for the temporal resolution. From the fit with this simple model (dashed lines in Fig. 2) we obtain  $\tau_{\text{icoh}} \approx 500$  fs. Indeed, these two processes seem to be required to consistently describe both  $\Delta I_{\text{CDW}}(t_d)$  and  $\Delta I_{\text{Bragg}}(t_d)$ . It is due to  $\tau_{\text{coh}} < \tau_{\text{icoh}}$  that  $I_{\text{CDW}}$  reaches its minimum several 100 fs later than the maximum in  $I_{\text{Bragg}}$ , see solid and dashed vertical lines in Figure 2 (b) and (c). Interestingly, this delay is becoming larger with increasing  $F$ , which can be attributed to different  $F$ -dependence of the two processes.

The observation that the complete C-IC phase transition is achieved only after a substantial part of the ab-

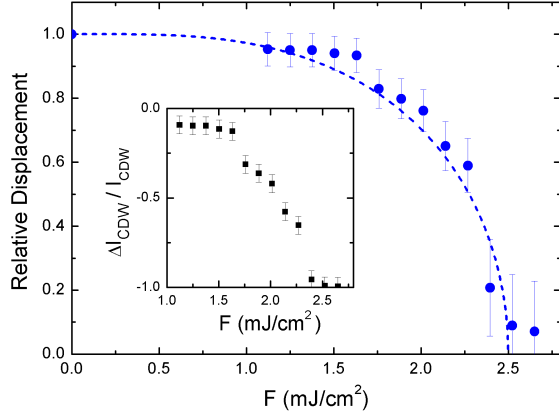


FIG. 3. Fluence dependence of transient PLD displacement at  $t_d = 1$  ps relative to its unperturbed value. The data are fit with the BCS function, where temperature was replaced by fluence as control parameter. The insert shows the corresponding changes in  $I_{\text{CDW}}$ .

sorbed energy is transferred to lattice vibrations via e-ph relaxation suggests that the optically induced phase transition relies not only on launching the amplitude modes via electronically driven change of the interatomic potential, but also on exciting specific strongly coupled lattice modes. Thus, the photoinduced phase transition seems not to be purely electronically driven. Further support for the importance of strong e-ph coupling comes from the fact that the optically delivered energy required to fully drive the C-IC phase transition corresponds well to the energy required to heat up the sample to  $T_c = 410$  K. Using the measured absorbed energy and the specific heat of  $c_p = 85.7$  J/(mole K) [32] we indeed obtain a temperature increase of  $\sim 110$  K at the critical fluence  $F_c = 2.5$  mJ/cm<sup>2</sup>, see Fig. 3. This finding is in agreement with previous studies on a quasi-1D CDW in  $\text{K}_{0.3}\text{MoO}_3$  [12] and  $1\text{T-TaS}_2$  [23], while in  $1\text{T-TiSe}_2$  the absorbed optical energy density required to drive the phase transition was reported to be lower than the corresponding thermal one [24].

In the perturbative regime at  $F < 2.5$  mJ/cm<sup>2</sup> the CDW reformation is found to proceed with the timescale  $\tau_{\text{rec}} \approx 150$  ps, see Fig. 2(c).  $\tau_{\text{rec}}$  is about two orders of magnitude larger than the observed recovery times in  $1\text{T-TaS}_2$  ( $\approx 4$  ps) [23] and  $1\text{T-TiSe}_2$  ( $\approx 1$  ps) [24]. Thus, the CDW in  $4\text{H}_b\text{-TaSe}_2$  seems far less cooperative than in the two above mentioned dichalcogenides. The most obvious difference between the polytypes is the interplane coupling between the  $T$  layers, which is strongly reduced in  $4\text{H}_b\text{-TaSe}_2$  due to the intermediate  $H$  layers which are not contributing to the CDW. The reduced coupling in  $4\text{H}_b\text{-TaSe}_2$  is demonstrated also by the reduction of the phase transition temperature from  $T_c = 473$  K for  $1\text{T-TaSe}_2$  to  $T_c = 410$  K [27]. In this respect the dramatically prolonged CDW recovery in  $4\text{H}_b\text{-TaSe}_2$  as opposed to the

other two  $1\text{T}$  dichalcogenides hints to the importance of a certain degree of three-dimensionality for the formation of CDW order in these systems. In other words, these results suggest that a purely two dimensional CDW order, as e.g. in a single  $T\text{-TaSe}_2$  layer, might not be possible.

In the regime above  $F > 2.5$  mJ/cm<sup>2</sup> where the CDW is completely suppressed, the CDW recovery proceeds on a much longer ( $> \text{ns}$ ) timescale. For this time delays the system can be described simply by an elevated temperature. Cooling is governed by the heat diffusion, which is slow due to the weak thermal coupling of the free standing film to the copper mesh.

To gain additional insights into the nature of the transient state, we performed a detailed study of the structural order parameter (the displacement amplitude) as a function of the excitation density. The displacement amplitude relative to the unperturbed state is extracted directly from the relative change in  $I_{\text{CDW}}$  (inset to Fig. 3), taking into account that  $I_{\text{CDW}} \propto (\mathbf{Q} \cdot \mathbf{A})^2$ , where  $\mathbf{Q}$  is the CDW wave vector and  $\mathbf{A}$  is the atomic displacement.

In thermal equilibrium the C-IC phase transition has been identified to be of a strong first order [27]. This is consistent with the  $F$ -dependence of  $I_{\text{CDW}}$  in a quasi-thermal equilibrium at  $t_d \approx 1$  ns, where a step like change between  $F = 2.3$  and  $2.6$  mJ/cm<sup>2</sup> is observed - see Fig. 2(c). The functional behavior of the order parameter at  $t_d = 1$  ps upon increasing  $F$  (Fig. 3) clearly shows a different character. Indeed, the order parameter ( $|\mathbf{A}|$ ) at  $t_d \approx 1$  ps can be very well fitted by the BCS functional form, characteristic for second order phase transitions. The dashed line in Fig. 3 is given by a well known analytic approximation to the BCS gap equation [33]: here instead of temperature  $T$  fluence  $F$  is used as a control parameter,  $\Delta/\Delta_0 = \tanh(1.78(F_c/F - 1)^{1/2})$ , with the critical fluence  $F_c = 2.5$  mJ/cm<sup>2</sup>. This clearly suggests a non-thermal character of the photoinduced state. Moreover, this observation could present an important clue for the theoretical understanding of interplay between electrons and lattice leading to the appearance of CDWs in layered dichalcogenides.

In conclusion, we have studied the structural order parameter dynamics in the CDW compound  $4\text{H}_b\text{-TaSe}_2$  using femtosecond electron diffraction. We show that the CDW is suppressed on the sub-ps timescale, launched by the electronically driven changes of the interatomic potential, and further enhanced by strongly coupled lattice modes generated via e-ph scattering. In the perturbative regime the CDW recovery time in  $4\text{H}_b\text{-TaSe}_2$  ( $\approx 150$  ps) is found to be two orders of magnitude larger than previously observed structural recovery times in similar transition-metal dichalcogenides. This observation highlights the importance of three-dimensionality for the existence of CDWs in layered compounds. Finally, the fluence dependence of the CDW order parameter showed, that the photoinduced ultrafast C-IC phase transition in  $4\text{H}_b\text{-TaSe}_2$  is of second order in contrast to a first order

thermally driven (slow) transition.

This work is based upon research supported by the South African Research Chair Initiative of the Department of Science and Technology and the National Research Foundation, the Alexander von Humboldt Foundation and Center for Applied Photonics at University of Konstanz. M. E. gratefully acknowledges a scholarship from Stiftung der Deutschen Wirtschaft (sdw). We acknowledge valuable discussions with A.S. Alexandrov, V.V. Kabanov, I.I. Mazin, K. Rossnagel and S. van Smaalen.

\*These authors contributed equally to this work.

- 
- [1] G. Gruner and A. Zettl, *Physics Reports* **119**, 117 (1985).
  - [2] R. Peierls, "Quantum Theory of Solids," Oxford University Press (1956).
  - [3] M. Johannes and I. Mazin, *Phys. Rev. B* **77**, 165135 (2008).
  - [4] L. Gor'kov, *Phys. Rev. B* **85**, 165142 (2012).
  - [5] K. Rossnagel, *J. Phys.: Condens. Matter* **23**, 213001 1 (2011).
  - [6] B. Burk and A. Zettl, *Phys. Rev. B* **46**, 9817 (1992).
  - [7] J. Lüdecke, S. van Smaalen, A. Spijkerman, J. de Boer, and G. Wiegers, *Phys. Rev. B* **59**, 6063 (1999).
  - [8] J. Demsar, L. Forró, H. Berger, and D. Mihailovic, *Phys. Rev. B* **66**, 041101 (2002).
  - [9] L. Perfetti, P. Loukakos, M. Lisowski, U. Bovensiepen, H. Berger, S. Biermann, P. Cornaglia, A. Georges, and M. Wolf, *Phys. Rev. Lett.* **97** (2006).
  - [10] H. Schäfer, V. Kabanov, M. Beyer, K. Biljakovic, and J. Demsar, *Phys. Rev. Lett.* **105**, 066402 (2010).
  - [11] F. Schmitt, P. S. Kirchmann, U. Bovensiepen, R. G. Moore, L. Rettig, M. Krenz, J. H. Chu, N. Ru, L. Perfetti, D. H. Lu, M. Wolf, I. R. Fisher, and Z.-X. Shen, *Science* **321**, 1649 (2008).
  - [12] A. Tomeljak, H. Schäfer, D. Städter, M. Beyer, K. Biljakovic, and J. Demsar, *Phys. Rev. Lett.* **102**, 066404 (2009).
  - [13] T. Rohwer, S. Hellmann, M. Wiesenmayer, C. Sohrt, A. Stange, B. Slomski, A. Carr, Y. Liu, L. M. Avila, M. Kalläne, S. Mathias, L. Kipp, K. Rossnagel, and M. Bauer, *Nature* **471**, 490 (2011).
  - [14] J. Petersen, S. Kaiser, N. Dean, A. Simoncig, H. Liu, A. Cavaleri, C. Cacho, I. Turcu, E. Springate, F. Frassetto, L. Poletto, S. Dhesi, H. Berger, and A. Cavalleri, *Phys. Rev. Lett.* **107**, 177402 (2011).
  - [15] D. Mihailovic, D. Dvorsek, V. V. Kabanov, J. Demsar, L. Forró, and H. Berger, *Appl. Phys. Lett.* **80**, 871 (2002).
  - [16] R. Yusupov, T. Mertelj, V. V. Kabanov, S. Brazovskii, P. Kusar, J.-H. Chu, I. R. Fisher, and D. Mihailovic, *Nature Physics* **6**, 681 (2010).
  - [17] K. Sokolowski-Tinten, C. Bloeme, J. Blums, A. Cavalleri, C. Dietrich, A. Tarasewitch, I. Uschmann, E. Förster, M. Kammler, M. Horn-von Hoegen, and D. von der Linde, *Nature* **422**, 287 (2003).
  - [18] D. M. Fritz, D. A. Reis, B. Adams, R. A. Akre, J. Arthur, C. Blome, P. H. Bucksbaum, A. L. Cavaleri, S. Engemann, S. Fahy, R. W. Falcone, P. H. Fuoss, K. J. Gaffney, M. J. George, J. Hajdu, M. P. Hertlein, P. B. Hillyard, M. Horn-von Hoegen, M. Kammler, J. Kaspar, R. Kienberger, P. Krejčík, S. H. Lee, A. M. Lindenberg, B. McFarland, D. Meyer, T. Montagne, E. D. Murray, A. J. Nelson, M. Nicoul, R. Pahl, J. Rudati, H. Schlarb, D. P. Siddons, K. Sokolowski-Tinten, T. Tschentscher, D. von der Linde, and J. B. Hastings, *Science* **315**, 633 (2007).
  - [19] P. Beaud, S. L. Johnson, E. Vorobeve, U. Staub, R. A. D. Souza, C. J. Milne, Q. X. Jia, and G. Ingold, *Phys. Rev. Lett.* **103**, 155702 (2009).
  - [20] B. Siwick, J. Dwyer, R. Jordan, and D. Miller, *Science* **302**, 1382 (2003).
  - [21] P. Baum, D.-S. Yang, and A. Zewail, *Science* **318**, 788 (2007).
  - [22] G. Sciaini and R. J. D. Miller, *Reports on Progress in Physics* **74**, 096101 (2011).
  - [23] M. Eichberger, H. Schäfer, M. Krumova, M. Beyer, J. Demsar, H. Berger, G. Moriena, G. Sciaini, and R. J. D. Miller, *Nature* **468**, 799 (2010).
  - [24] E. Möhr-Vorobeve, S. Johnson, P. Beaud, U. Staub, R. De Souza, C. Milne, G. Ingold, J. Demsar, H. Schaefer, and A. Titov, *Phys. Rev. Lett.* **117**, 036403 (2011).
  - [25] B. Brown and D. Beerntsen, *Acta Crystallographica* **18**, 31 (1965).
  - [26] J. A. Wilson, F. J. Di Salvo, and S. Mahajan, *Advances in Physics* **24**, 117 (1975).
  - [27] F. Di Salvo, D. Moncton, and J. Wilson, *Phys. Rev. B* **14**, 1543 (1976).
  - [28] M. Eichberger, M. Krumova, H. Berger, and J. Demsar, *Ultramicroscopy*, accepted for publication (2012).
  - [29] G. Kassier, K. Haupt, N. Erasmus, E. Rohwer, H. von Bergmann, H. Schwoerer, S. Coelho, and D. Aurret, *Rev. Sci. Instrum.* **81**, 105103 (2010).
  - [30] A. R. Beal, *Journal of Physics C: Solid State Physics* **11**, 4583 (1978).
  - [31] T. Nakashizu, T. Sekine, K. Uchinokura, and E. Matsuura, *Phys. Rev. B* **29**, 3090 (1984).
  - [32] A. Bolgar, Z. Trot'nnova, A. Blinder, and A. Yanaki, *Powder Metall. Met. Ceram.* **31**, 601 (1992).
  - [33] R. Meservey and B. Schwartz, in *Superconductivity*, Vol. 1, edited by R. Park (Marcel Dekker, New York, 1969) p. 117.